Interest Rate Model Documentation

Comprehensive Model Description, Assumptions, and Limitations

MUFG Securities EMEA plc

December 19, 2025

Contents

1 Finding 1: Absence of Pathwise Arbitrage-Free Term-Structure Dynamics

1.1 Finding Statement

The Interest Rate (IR) simulation model does not enforce pathwise arbitrage-free relationships across maturities. Each zero-rate maturity pillar is simulated as a distinct stochastic process, with cross-tenor dependence introduced exclusively via correlation between latent drivers. As a result, discount-factor multiplicative identities and forward-rate reconstruction conditions are not guaranteed to hold along individual Monte Carlo paths, particularly at long horizons or under elevated volatility regimes.

This limitation may lead to economically implausible curve shapes and dynamic inconsistencies in simulated interest-rate term structures.

1.2 Model Mechanics Leading to the Finding

1.2.1 Pillar-wise Stochastic Construction

In the implemented framework, each maturity pillar k of the ultimate base curve is simulated independently through a shifted exponential Vasicek-type construction:

$$Y_k(t) = \big(g_k(t) + s_k\big) \exp\big(X_k(t) - \tfrac{1}{2} v_k^2(t)\big) - s_k, \tag{1}$$

where:

- $X_k(t)$ follows an Ornstein–Uhlenbeck process,
- $g_k(t)$ is a deterministic mean function calibrated from the initial forward-forward curve,
- s_k is a shift ensuring numerical stability,
- $v_k^2(t) = \mathrm{Var}[X_k(t)]$.

Each pillar has its own stochastic driver X_k; dependence across maturities is introduced solely through correlation of the Brownian motions driving X_k.

1.2.2 Absence of Term-Structure Arbitrage Constraints

The model does not impose:

- a short-rate representation,
- an instantaneous forward-rate framework,
- nor Heath–Jarrow–Morton (HJM) drift restrictions linking volatilities and drifts across maturities.

Consequently, while the model is marginally consistent with the initial yield curve in expectation, it does not guarantee joint consistency of the full curve along simulated paths.

1.3 Theoretical Corroboration

1.3.1 Arbitrage-Free Requirement in Term-Structure Models

In arbitrage-free short-rate or HJM frameworks, discount factors satisfy the pathwise multiplicative identity:

$$DF(t, t+T) = DF(t, t+u) \cdot DF(t+u, t+T), \qquad \forall\ 0 < u < T, \tag{2}$$

since each discount factor is an exponential of the integral of a single underlying short rate over disjoint time intervals.

Equivalently, instantaneous forward rates $f(t,T)$ must satisfy HJM drift restrictions of the form:

$$\alpha(t,T) = \sigma(t,T) \int_t^T \sigma(t,u)\, du, \tag{3}$$

ensuring the absence of arbitrage under the risk-neutral measure.

1.3.2 Why the Implemented Model Violates These Identities

In the current model:

- $DF(t, t+T)$ is inferred from the simulated zero rate $Y_T(t)$,
- $DF(t+u, t+T)$ is inferred from an independently simulated curve at time $t+u$,
- no structural constraint enforces multiplicative consistency between the two.

As a result, discount factors reconstructed at different times along a path need not satisfy the multiplicative identity, even in the absence of interpolation effects.

1.4 Practical Implications for PFE

The absence of pathwise arbitrage-free dynamics may result in:

- Static inconsistencies, such as non-monotone discount factors or implausible forward-rate shapes at a given time point.
- Dynamic inconsistencies, where long-horizon discount factors do not match the compounded effect of shorter-dated discount factors along the same path.
- Potential bias in exposure profiles, particularly for long-dated interest rate derivatives whose valuation depends on the joint evolution of the full curve.

The materiality of these effects depends on portfolio maturity, volatility regime, and reliance on pathwise discounting.

1.5 Validation Tests and Diagnostics

1.5.1 Test 1A: Static Discount-Factor Monotonicity

Objective Verify the absence of static arbitrage at each simulation time by checking monotonicity of implied discount factors.

Definition For each path p, time t_i, and maturity pillar M_k:

$$DF(t_i, t_i + M_k) := \exp\big(-Y_k(t_i)\, M_k\big). \tag{4}$$

The following condition should hold:

$$DF(t_i, t_i + M_{k+1}) \leq DF(t_i, t_i + M_k), \qquad \forall k. \tag{5}$$

Implementation Discount factors are computed from simulated zero rates and violations are identified where discount factors increase with maturity.

Outputs

- Fraction of violated (p, t, k) triplets.
- Maximum severity of monotonicity breaches.
- Heatmap of violation frequency by time and maturity interval.

1.5.2 Test 1B: Forward-Rate Reconstruction Sanity

Objective Assess whether implied forward rates between maturity pillars remain stable and economically plausible.

Definition For $M_i < M_j$, the implied forward rate is:

$$F_{i,j}(t) = \frac{Y_j(t)M_j - Y_i(t)M_i}{M_j - M_i}. \tag{6}$$

Diagnostics

- Distribution of forward rates by maturity bucket.
- Time evolution of percentile bands.
- Curvature metrics based on second finite differences.

1.5.3 Test 1C: Pathwise Discount-Factor Multiplicative Identity

Objective Directly quantify the failure of pathwise arbitrage-free discounting.

Definition For a simulation time step u and maturity T:

$$\text{Wedge}(t, u, T) = \log DF(t, t+T) - \log DF(t, t+u) - \log DF(t+u, t+T). \tag{7}$$

In an arbitrage-free model, this quantity should be approximately zero.

Implementation Discount factors are inferred from simulated curves at times t and $t + u$, and the wedge is computed pathwise.

Outputs

- Wedge distributions by maturity.
- Mean and percentile bands over time.
- Fraction of paths exceeding tolerance thresholds.

1.6 Illustrations

The following figures are produced to support validation and governance:

- Discount-factor monotonicity violation heatmaps.
- Forward-rate curvature diagnostics across maturities.
- Wedge distribution histograms for long-dated maturities.
- Wedge magnitude as a function of maturity horizon.

1.7 Conclusion

The absence of pathwise arbitrage-free term-structure dynamics is an inherent structural feature of the pillar-based IR simulation model and not an implementation defect.

While the model remains suitable for PFE applications where marginal distributions dominate risk assessment, the limitation must be explicitly documented, quantitatively monitored, and benchmarked against arbitrage-free frameworks such as HJM or multi-factor short-rate models to assess materiality for specific portfolios.

1.8 Finding 1-Illustration — Absence of Pathwise Arbitrage-Free Term-Structure Dynamics

This section presents quantitative diagnostics and illustrative evidence supporting Finding 1, namely that the Interest Rate (IR) simulation model does not enforce pathwise arbitrage-free term-structure dynamics. The diagnostics focus on static no-arbitrage conditions, cross-tenor smoothness, and pathwise discount-factor consistency, and are benchmarked against an arbitrage-free Hull–White one-factor (HW1F) model.

1.8.1 Definition of the kink index (cross-tenor smoothness diagnostic)

Let the simulated zero-rate curve at simulation time t be defined on a discrete set of maturity pillars $\{M_k\}_{k=0}^{K-1}$, with corresponding zero rates $\{Y_k(t)\}_{k=0}^{K-1}$.

We define the first finite difference (local slope proxy) as:

$$\Delta Y_k(t) = Y_{k+1}(t) - Y_k(t),$$

and the second finite difference (local curvature proxy) as:

$$\Delta^2 Y_k(t) = Y_{k+1}(t) - 2Y_k(t) + Y_{k-1}(t), \qquad k = 1, \ldots, K-2.$$

The *kink index* at time t is defined as:

$$\boxed{\text{Kink}(t) = \max_{k=1,\ldots,K-2} \left|\Delta^2 Y_k(t)\right|.}$$

The kink index quantifies the maximum local curvature across adjacent maturity pillars. Large values indicate abrupt changes in slope between neighbouring tenors and reflect reduced cross-tenor coherence and economically implausible local deformations of the simulated term structure.

1.8.2 Static discount-factor monotonicity

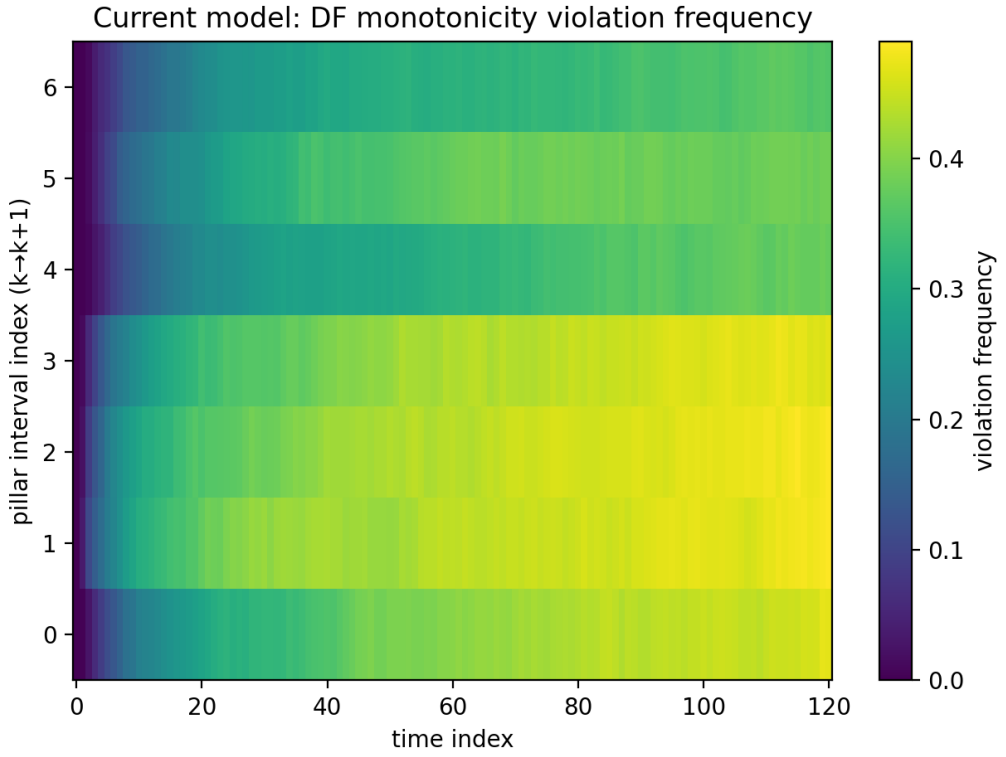

Figure 1: Current model: frequency of discount-factor monotonicity violations across time and maturity pillar intervals.

Figure 1 reports the frequency with which the static no-arbitrage condition

$$DF(t, T_{k+1}) \leq DF(t, T_k)$$

is violated across simulation time and adjacent maturity pillars under the current model. Violations are observed to increase both with simulation horizon and with maturity, reaching frequencies in excess of 40–50% for some pillar intervals at longer horizons. This indicates that the simulated curve snapshots are not systematically decreasing in maturity and that static arbitrage conditions are not structurally enforced.

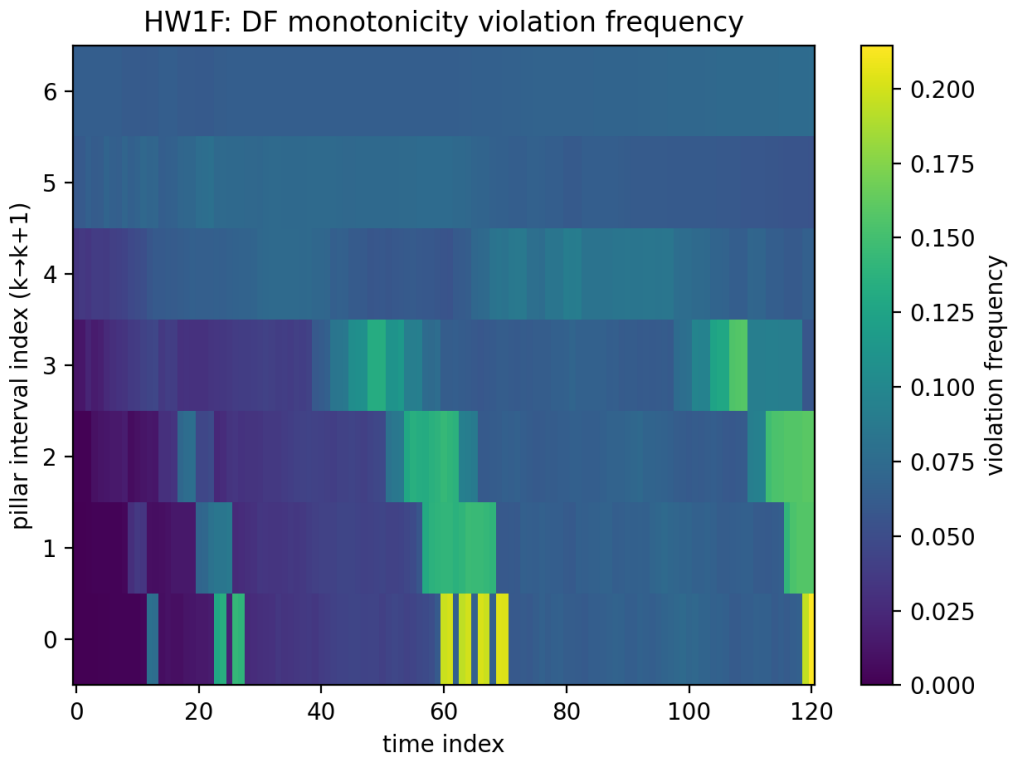

Figure 2: HW1F benchmark: frequency of discount-factor monotonicity violations.

In contrast, Figure 2 shows that under the HW1F benchmark model, monotonicity violations are rare, sporadic, and of limited magnitude. This behaviour is consistent with numerical discretisation effects rather than structural arbitrage.

1.8.3 Cross-tenor smoothness and kink diagnostics

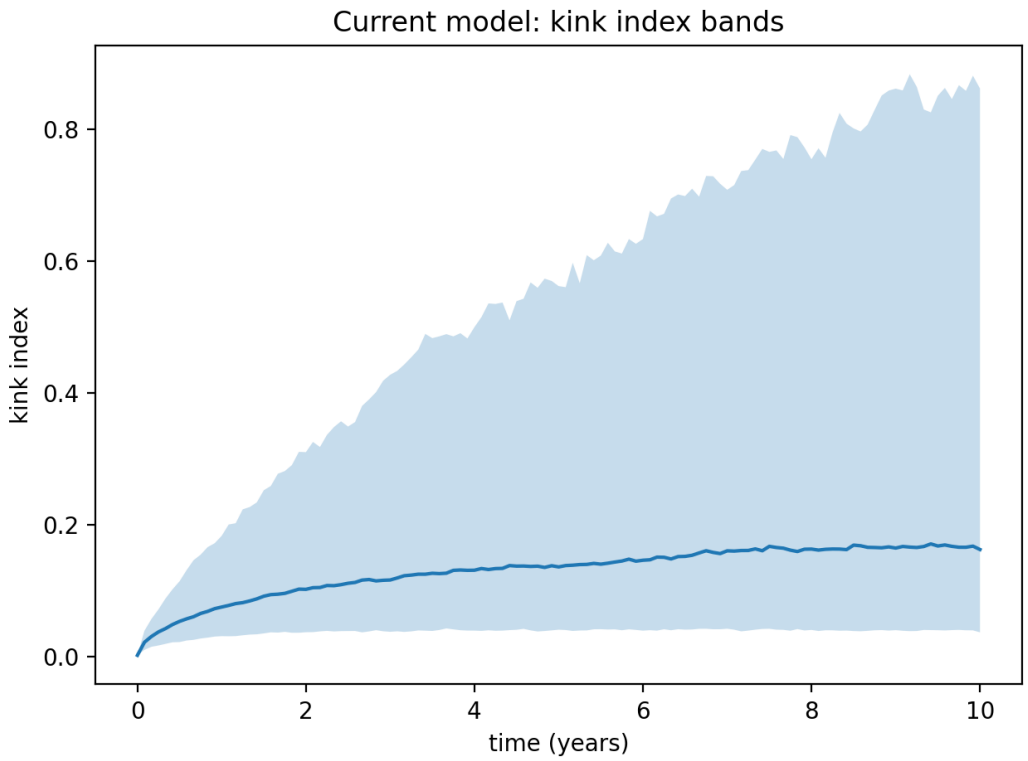

Figure 3: Current model: kink index bands (median and 5th–95th percentiles) as a function of simulation time.

Figure 3 reports the evolution of the kink index under the current model. The median kink index increases steadily with time, while the upper quantiles exhibit pronounced growth, reaching large values at longer horizons. The widening dispersion indicates that local curve smoothness deteriorates as stochastic variance accumulates, reflecting the absence of structural constraints linking adjacent maturity pillars.

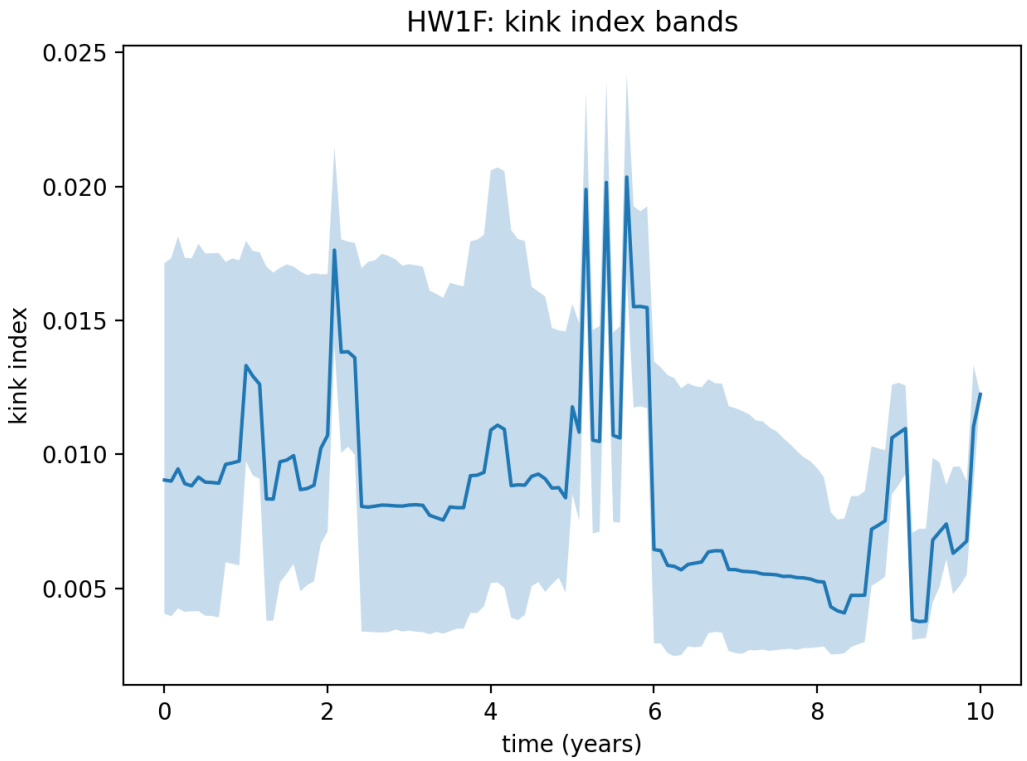

Figure 4: HW1F benchmark: kink index bands.

Under the HW1F benchmark (Figure 4), the kink index remains low, stable, and tightly distributed over time. This reflects the fact that the entire curve is generated from a single latent short-rate factor, ensuring smooth and coherent cross-tenor dynamics by construction.

1.8.4 Pathwise discount-factor multiplicative consistency

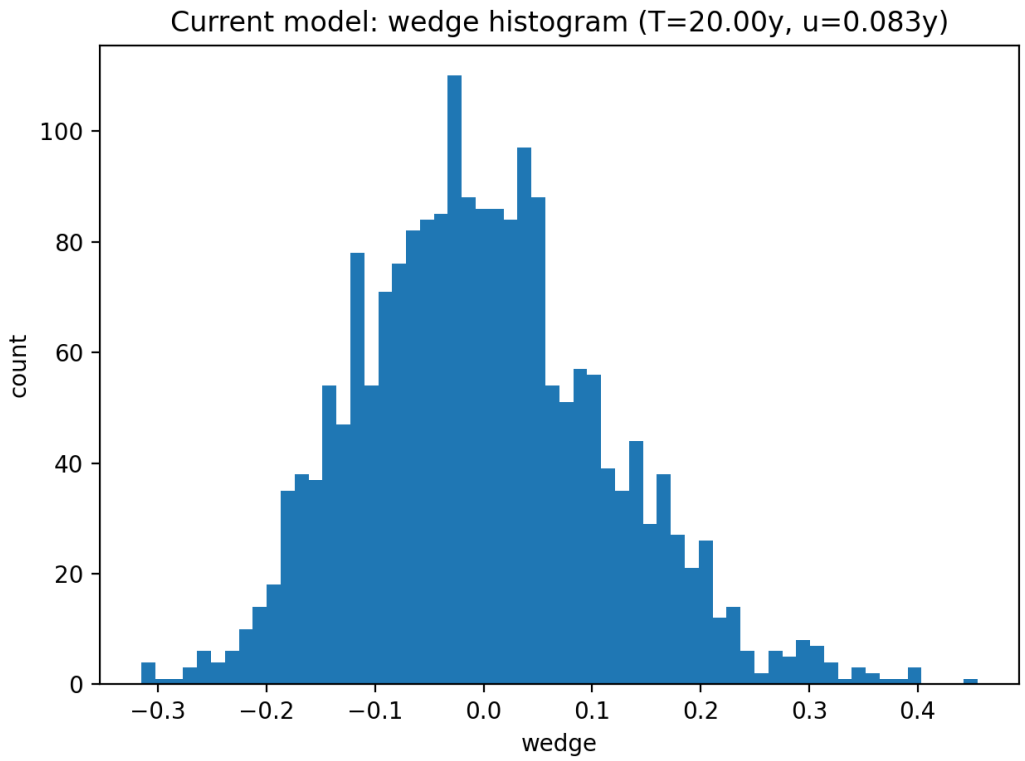

Figure 5: Current model: distribution of the pathwise discount-factor wedge for $T = 20$ years and $u \approx 1$ month.

Figure 5 displays the distribution of the pathwise discount-factor wedge:

$$\log DF(t, T) - \log DF(t, u) - \log DF(t + u, T - u),$$

under the current model. The distribution is wide and significantly dispersed away from zero, indicating substantial violations of the multiplicative discount-factor identity along individual simulation paths.

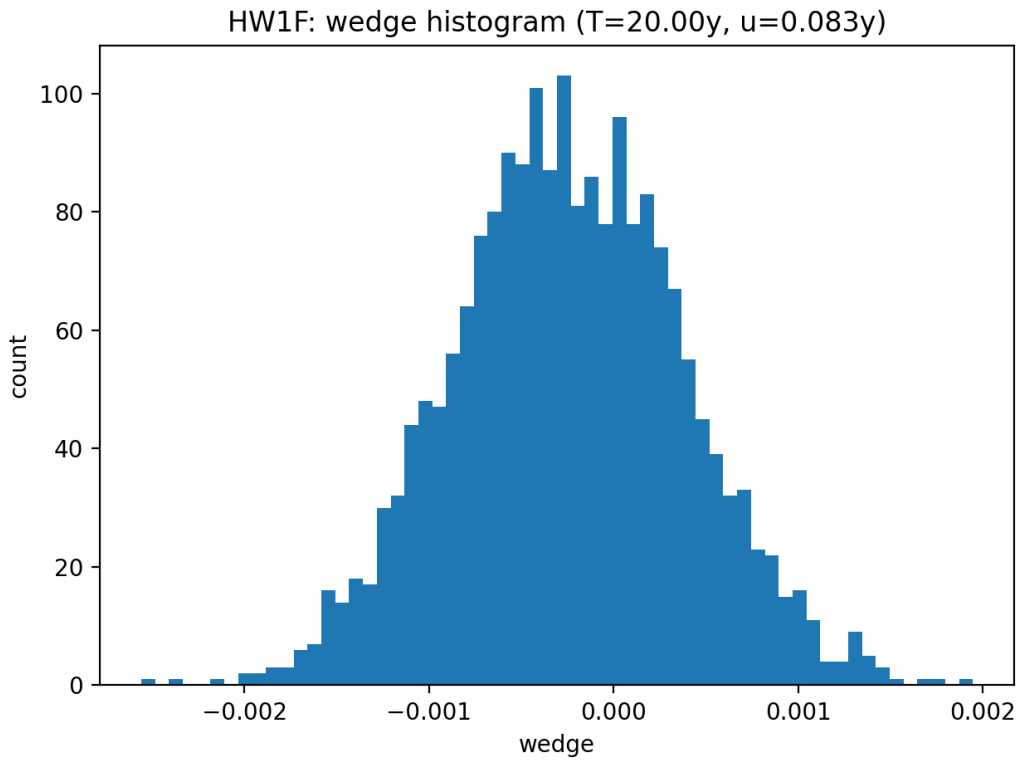

Figure 6: HW1F benchmark: distribution of the pathwise discount-factor wedge.

By contrast, the HW1F benchmark (Figure 6) exhibits a tightly concentrated wedge distribution centred near zero, with magnitudes several orders of magnitude smaller, consistent with numerical approximation error only.

1.8.5 Wedge severity as a function of maturity

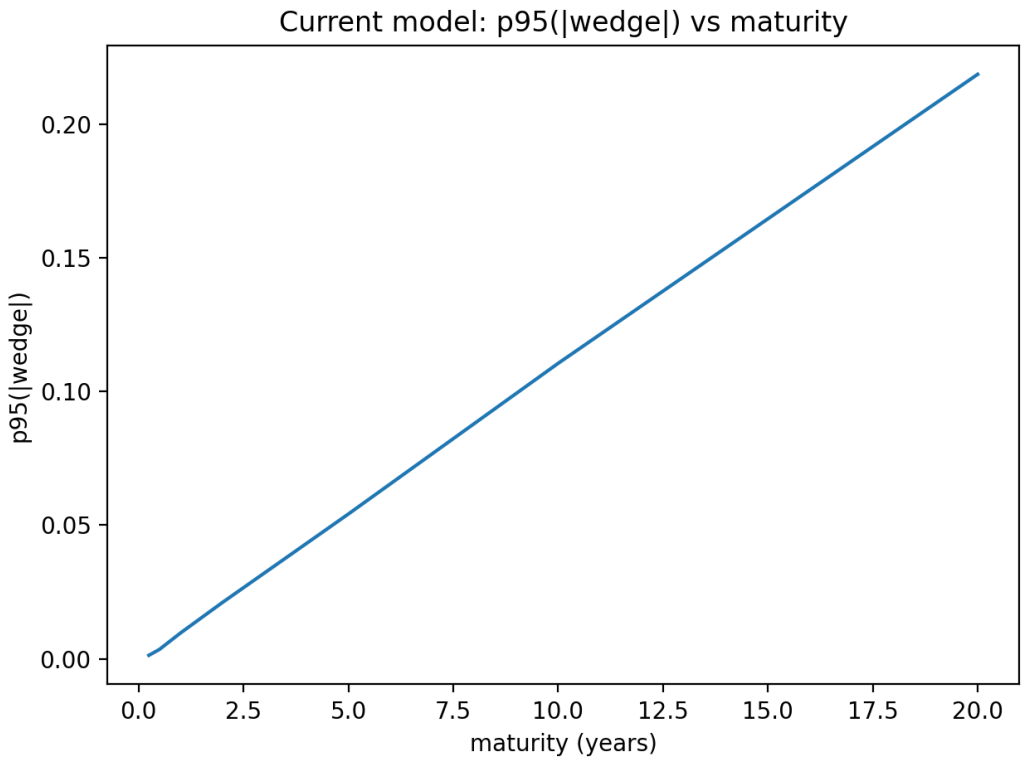

Figure 7: Current model: 95th percentile of |wedge| as a function of maturity.

Figure 7 shows that the severity of pathwise discount-factor inconsistencies increases approximately linearly with maturity under the current model, reaching material levels for long-dated tenors. This indicates that arbitrage violations accumulate with horizon and disproportionately affect long-dated exposures.

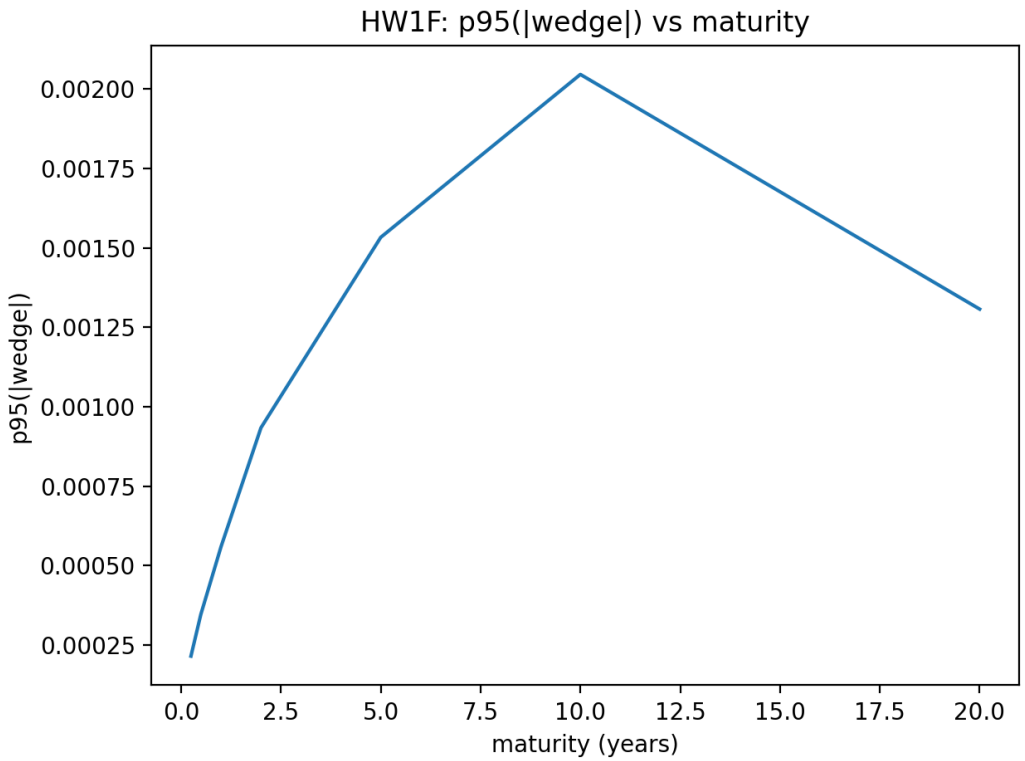

Figure 8: HW1F benchmark: 95th percentile of |wedge| versus maturity.

The HW1F benchmark exhibits uniformly low wedge magnitudes across maturities (Figure 8), confirming that no structural amplification of inconsistencies occurs under an arbitrage-free short-rate framework.

1.8.6 Conclusion

The diagnostics presented above provide consistent and complementary evidence that the current IR simulation model does not enforce pathwise arbitrage-free term-structure dynamics. Violations are systematic, horizon-dependent, and materially larger than those observed under an arbitrage-free benchmark model. While this behaviour is a known and documented consequence of the model design, it represents a structural limitation that must be monitored, benchmarked, and appropriately controlled when assessing long-dated exposure profiles.